Acta Cryst E CRYSTALLOGRAPHIC COMMUNICATIONS

ISSN 2056-9890

Synthesis, crystal structure and Hirshfeld surface analysis of (4-methylphenyl)[1-(pentafluorophenyl)-5-(trifluoromethyl)-1*H*-1,2,3-triazol-4-yl]methanone

Nazariy T. Pokhodylo,[a]* Yurii Slyvka,[b] Evgeny Goreshnik[c] and Roman Lytvyn[a]

[a]Department of Organic Chemistry, Ivan Franko National University of Lviv, Kyryla i Mefodiya, 6, Lviv, 79005, Ukraine, [b]Department of Inorganic Chemistry, Ivan Franko National University of Lviv, Kyryla i Mefodiya, 6, Lviv, 79005, Ukraine, and [c]Department of Inorganic Chemistry and Technology, Jozef Stefan Institute, Jamova 39, SI-1000 Ljubljana, Slovenia. *Correspondence e-mail: pokhodylo@gmail.com

Received 20 September 2021
Accepted 28 September 2021

Edited by W. T. A. Harrison, University of Aberdeen, Scotland

Keywords: crystal structure; 1,2,3-triazole; Hirshfeld surface analysis.

CCDC reference: 2112438

Supporting information: this article has supporting information at journals.iucr.org/e

The title compound, $C_{17}H_7F_8N_3O$, was obtained *via* the reaction of 1-azido-2,3,4,5,6-pentafluorobenzene with 4,4,4-trifluoro-1-(*p*-tolyl)butane-1,3-dione using triethylamine as a base catalyst and solvent. The dihedral angles between the pentafluorophenyl (*A*), triazole (*B*) and *p*-tolyl (*C*) rings are *A*/*B* = 62.3 (2), *B*/*C* = 43.9 (3) and *A*/*C* = 19.1 (3)°. In the crystal, the molecules are linked by C—H···F and C—H···O hydrogen bonds as well as by aromatic π–π stacking interactions into a three-dimensional network. To further analyse the intermolecular interactions, a Hirshfeld surface analysis was performed.

1. Chemical context

Compounds with perfluoroaromatic motifs are of interest for the design of fluorescence materials, including their application in optoelectronic devices (Funabiki *et al.*, 2021; Feng *et al.*, 2021; Moseev *et al.*, 2019; Kandhadi *et al.*, 2018; Lukeš *et al.*, 2016; Wang *et al.*, 2013; Matsui *et al.*, 2008). For instance, the perfluorobiphenyl moiety was used as an electron acceptor for new donor–acceptor compounds with thermally activated delayed fluorescence (TADF) applied for the fabrication of TADF-based OLEDs (Danyliv *et al.*, 2021; Hladka *et al.*, 2018). On the other hand, 1,2,3-triazoles, as a result of their electron-accepting properties, are widely used in the design of organic phosphors (Gavlik *et al.*, 2017; Fernández-Hernández *et al.*, 2013; Tomkute-Luksiene *et al.*, 2013; Ichikawa *et al.*, 2011). Recently, a series of 3,6-bis(4-triazolyl)pyridazines equipped with terminal phenyl substituents with varying degrees of fluorination were synthesized and proposed to be used as electron-transporting/hole-blocking materials in organic electronics (Birkenfelder *et al.*, 2017). In view of this, we decided to combine these two fragments in order to construct new molecular scaffolds of compounds that have the potential for use in optoelectronic devices.

Despite the prospects of using 1-(perfluorophenyl)-1*H*-1,2,3-triazole in the creation of phosphor materials, the paths of their synthesis are poorly studied. It is known that azides are convenient precursors of 1,2,3-triazoles. A literature survey showed limited data on the reaction of perfluorophenylazide in the synthesis of 1,2,3-triazoles. The reactions of such azides with acetylenes, which occur as a 1,3-dipolar

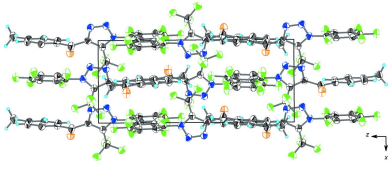

cycloaddition, are primarily studied. For example, perfluorophenylazide was studied in the copper-catalysed azide–alkyne cycloaddition (CuAAC) click reaction with propargyl alcohol (Lavoie *et al.*, 2017), 5-chloropent-1-yne and 6-chlorohex-1-yne (Berry *et al.*, 2014), trimethyl[(perfluorophenyl)ethynyl]silane (Lu *et al.*, 2012), iodoethynylarenes (Maugeri *et al.*, 2016), 4-ethynylphospholo[3,2-*b*:4,5-*b*′]dithiophene 4-oxide (He, Zhang *et al.*, 2013), [4-(iodoethynyl)phenyl]diphenylphosphine oxide (Maugeri *et al.*, 2017), 2-ethynylpyridine (Liu *et al.*, 2011), bis-alkynes (Milo *et al.*, 2015) and 2,8-diethynyl-5-phenyl-4*H*-phosphepino[4,3-*b*:5,6-*b*′]dithiophene-4,6(5*H*)-dione (He, Borau-Garcia *et al.*, 2013). The CuAAC reaction of perfluorophenylazide was used for the synthesis and bioactivity of phthalimide analogues as potential drugs to treat schistosomiasis (Singh *et al.*, 2020) and for identification of sialoside analogues for siglec-based cell targeting (Rillahan *et al.*, 2012). Moreover, the 1,3-dipolar cycloaddition of perfluorinated aryl azides with enamines and strained dipolarophiles has been studied (Xie *et al.*, 2015). Additionally, non-catalytic Huisgen (3 + 2) cycloaddition of perfluorophenylazide with ethyl propiolate and a one-pot tandem Sonogashira cross-coupling/CuAAC reaction were studied (Kloss *et al.*. 2011). Conversely, for the synthesis of fully substituted 1,2,3-triazoles, Dimroth-type reactions are the most convenient. However, there is only one example of base-promoted cyclization of perfluorophenylazide with methylene active ketones (Dimroth-type reaction) in the triazole synthesis. Thus, by the reaction of perfluorophenylazide with acetylacetone in $CHCl_3$ under Et_3N and DBU catalysis, 1,2,3-triazoles were formed in 57% yield (Shafran *et al.*, 2019). It should be noted that the classical conditions of the Dimroth reaction are MeONa/MeOH (Krivopalov *et al.*, 2005). Such conditions are suitable for the rapid formation of polyheterocyclic 1,2,3-triazole derivatives *via* a domino reaction (Pokhodylo & Shyyka, 2017p; Pokhodylo *et al.*, 2014), but for reagents with labile functional groups (Pokhodylo *et al.*, 2018, 2020) or to avoid concurrent Regitz diazotransfer reaction (Pokhodylo & Obushak, 2019), mild bases such as K_2CO_3 (Pokhodylo *et al.*, 2017) or organic bases (Et_3N, DBU, pyrrolidine) are more suitable (Blastik *et al.*, 2018; Ramachary *et al.*, 2008; Danence *et al.*, 2011). Furthermore, it has been shown that mild bases Et_3N could be used for regioselective introduction of strongly electron-withdrawing groups such as trifluoroiodomethyl (CF_3) in the 1,2,3-triazole ring in the reaction with asymmetric 1,3-diketones (Rozin *et al.*, 2012).

Taking into account the above facts, in this work, the title compound, (I), was obtained and its crystal structure determined.

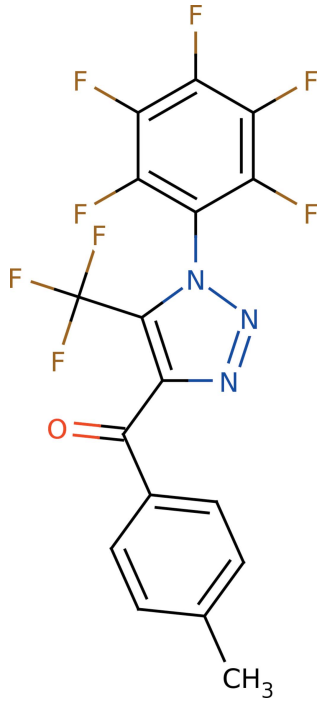

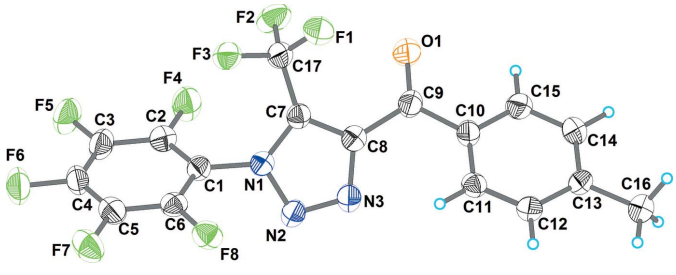

Figure 1
The molecular structure of (I) with displacement ellipsoids drawn at the 50% probability level.

2. Structural commentary

The title compound crystallizes in the non-centrosymmetric space group $P2_12_12_1$, with one molecule in the asymmetric unit. As shown in Fig. 1, it is constructed from three aromatic rings (C10–C15 4-methylphenyl, C1–C6 pentafluorophenyl and C7/C8/N1/N2/N3 triazole rings). The pentafluorophenyl ring and the heterocyclic ring are twisted relative to each other by 62.3 (2)° because of the significant steric hindrance of the trifluoromethyl group attached to C7. This dihedral angle is significantly smaller than the angle of 87.1° between the 4-nitrophenyl and triazole rings in the structure of 1-[5-methyl-1-(4-nitrophenyl)-1*H*-1,2,3-triazol-4-yl]ethanone (VI) (Vinutha *et al.*, 2013) but considerably larger than the analogous angle between aromatic rings in the structures of 3-(4-fluorophenyl)-1-[1-(4-fluorophenyl)-5-methyl-1*H*-1,2,3-triazol-4-yl]prop-2-en-1-one (39.6°; El-Hiti *et al.*, 2018), (4-methylphenyl)(5-methyl-1-phenyl-1*H*-1,2,3-triazol-4-yl)methanone (44.5°; Li *et al.*, 2014), 1-[1-(4-chlorophenyl)-5-methyl-1*H*-1,2,3-triazol-4-yl]ethanone (45.6°) and 1-[1-(4-bromophenyl)-5-methyl-1*H*-1,2,3-triazol-4-yl]ethanone (47.1°) (Zeghada *et al.*, 2011). The carbonyl group of the title compound is not in the plane of the adjacent aromatic rings: the C7—C8—C9—O1 and C15—C10—C9—O1 torsion angles are −25.4 (9) and −16.8 (9)°, respectively]. The 4-methylphenyl and triazole rings are twisted relative to each other by 43.9 (2)° and the 4-methylphenyl and pentafluorophenyl rings by 19.1 (3)°.

Table 1
Hydrogen-bond geometry (Å, °).

D—H···A	D—H	H···A	D···A	D—H···A
C11—H11···F3^{i}	0.95	2.49	3.155 (5)	127
C15—H15···F3^{ii}	0.95	2.61	3.463 (6)	149
C16—H16*A*···F2^{iii}	0.98	2.57	3.054 (6)	111
C16—H16*A*···O1^{iii}	0.98	2.54	3.505 (6)	167

Symmetry codes: (i) $x+\frac{1}{2}, -y+\frac{1}{2}, -z+1$; (ii) $-x+\frac{1}{2}, -y+1, z+\frac{1}{2}$; (iii) $-x+1, y-\frac{1}{2}, -z+\frac{3}{2}$.

3. Supramolecular features

As shown in Fig. 2 and listed in Table 1, the crystal structure of (I) features several weak intermolecular interactions. The hydrogen atoms of the 4-methylphenyl ring are involved in C—H···F hydrogen bonding with the trifluoromethyl substituents of adjacent molecules, while a hydrogen atom of the methyl group forms a C—H···O hydrogen bond with the carbonyl O atom of another adjacent molecule. The 4-methylphenyl and pentafluorophenyl rings of adjacent molecules are also involved into face-to-face π–π stacking interaction with a centroid–centroid separation of 3.783 (6) Å, while at the same time the triazole rings are involved into edge-to-face aromatic interactions at 3.218 (6) Å. The molecules are linked by the above-mentioned intermolecular interactions into a three-dimensional network (Fig. 3).

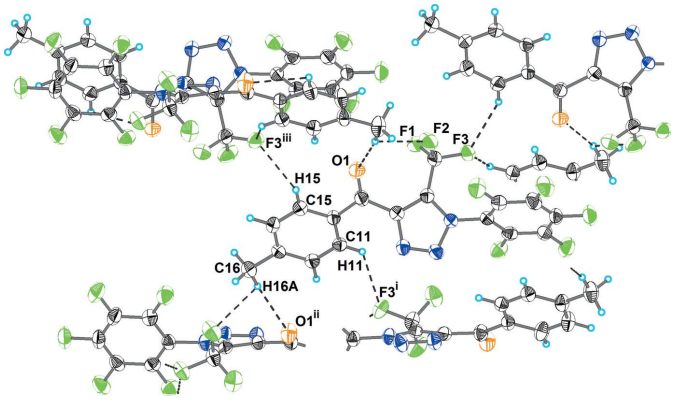

Figure 2
The hydrogen bonding of molecules in (I). Hydrogen bonds are shown as dashed lines. The symmetry codes are as in Table 1.

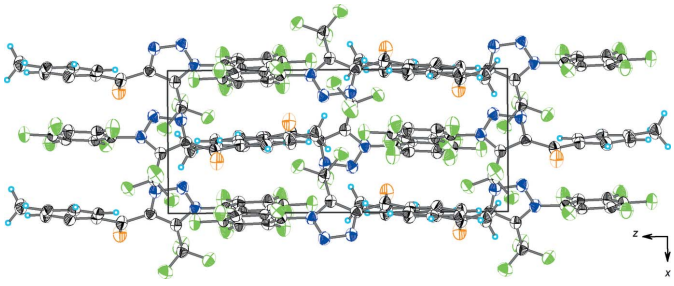

Figure 3
A view along the *b*-axis direction of the crystal packing of (I).

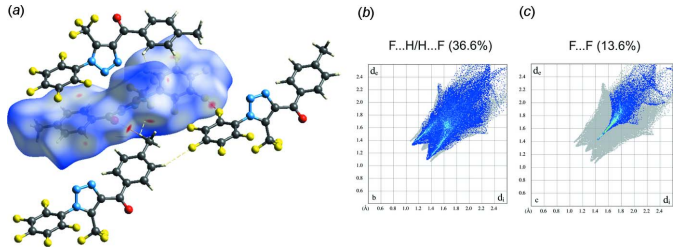

Figure 4
(*a*) Hirshfeld surface for (I) mapped with d_{norm} over the range −0.12 to 1.53 a.u. showing C—H···O and C—H···F hydrogen-bonded contacts as well as F···F contacts. Fingerprint plots resolved into (*b*) F···H/H···F and (*c*) F···F contacts. Neighbouring molecules associated with close contacts are also shown.

4. Hirshfeld surface analysis

Hirshfeld surface analysis was used to analyse the various intermolecular interactions in (I), through mapping the normalized contact distance (d_{norm}) using *CrystalExplorer* (Turner *et al.*, 2017; Spackman & Jayatilaka, 2009). The most prominent interactions (bifurcated interactions of atom H16*A* of the methyl group with the carbonyl group O atom and the fluorine atom of the trifluoromethyl substituent of neighbouring molecules, as well as the F···F interaction between neighbouring pentafluorophenyl rings) can be seen in the Hirshfeld surface plot as red areas (Fig. 4). Fingerprint plots were produced to show the intermolecular surface bond distances with the regions highlighted for F···H/H···F and F···F contacts interactions (Fig. 4). The contribution to the surface area for such contacts are 36.6% and 13.6%, respectively. The contribution to the surface area for O···H/H···O and H···H contacts are 4.6% and 5.7%, respectively.

5. Database survey

The most closely related compounds, containing a similar 1-aryl-1*H*-1,2,3-triazole-4-carbonyl skeleton to the title compound but with different substituents on the carbonyl group are: 2,2′-(quinoxaline-2,3-diyldisulfanediyl)bis{1-[5-methyl-1-(4-methylphenyl)-1*H*-1,2,3-triazol-4-yl]ethan-1-one} (II) [Cambridge Structural Database (Version 2021.1; Groom *et al.*, 2016) refcode ETUVEX; Mohamed *et al.*, 2021], 4-(4-acetyl-5-methyl-1*H*-1,2,3-triazol-1-yl)benzonitrile (III) (SILBOH; Zukerman-Schpector *et al.*, 2018), 1-[5-methyl-1-(4-methylphenyl)-1*H*-1,2,3-triazol-4-yl]ethan-1-one (IV) (LEMSUU; El-Hiti *et al.*, 2017), 3-(4-fluorophenyl)-1-[1-(4-fluorophenyl)-5-methyl-1*H*-1,2,3-triazol-4-yl]prop-2-en-1-one (V) (MESTAI; El-Hiti *et al.*, 2018), 1-[5-methyl-1-(4-nitrophenyl)-1*H*-1,2,3-triazol-4-yl]ethanone (VI) (QIRQOZ; Vinutha *et al.*, 2013), 2-bromo-1-[1-(4-bromophenyl)-5-methyl-1*H*-1,2,3-triazol-4-yl]ethanone (VII) (XODSAM; Bunev *et al.*, 2014), (4-methylphenyl)(5-methyl-1-phenyl-1*H*-1,2,3-triazol-4-yl)methanone (VIII) (COCYAW; Li *et al.*, 2014), (2*E*)-3-(4-fluorophenyl)-1-[5-methyl-1-(4-methylphen-

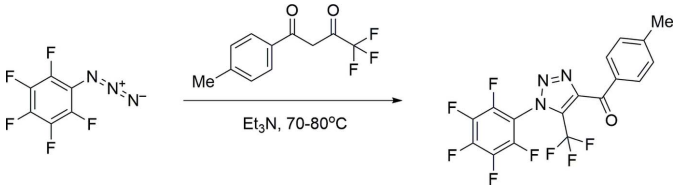

Figure 5
Synthesis scheme for (I)

yl)-1*H*-1,2,3-triazol-4-yl]prop-2-en-1-one (IX) (IDITUM; Abdel-Wahab *et al.*, 2013), 1-[1-(4-chlorophenyl)-5-methyl-1*H*-1,2,3-triazol-4-yl]ethanone (X) (ISOBUO; Zeghada *et al.*, 2011) and 1-[1-(4-bromophenyl)-5-methyl-1*H*-1,2,3-triazol-4-yl]ethanone (XI) (ISOCAV; Zeghada *et al.*, 2011).

Compounds (V), (IX), (X) and (XI) crystallize in the triclinic crystal system in space group $P\overline{1}$. Compounds (II), (III) and (IV), (VIII) crystallize in the monoclinic crystal system with space groups $P2_1/n$ and $P2_1/c$, respectively, while compound (VII) is found in the monoclinic crystal system, space group *Pn*. Compound (VI) crystallizes in the orthorhombic crystal system in non-centrosymmetric space group $Pca2_1$. Structures (V), (VI) and (VII) contain two crystallographically independent molecules. The aryl and triazole rings in (VI) are twisted relative to each other by 87.1 and 38.2° in the two crystallographically independent molecules. In compounds (III), (IV) and (IX), the analogous angles between the aromatic rings are 54.7, 50.1 and 51.8°, respectively.

6. Synthesis and crystallization

A number of experimental conditions described previously were investigated for the synthesis of the title compound (Shafran *et al.*, 2019; Pokhodylo *et al.*, 2017; Blastik *et al.*, 2018; Rozin *et al.*, 2012). However, it was possible to obtain the target product only in the case of the protocol proposed by Rozin *et al.* (2012). The synthesis scheme is shown in Fig. 5.

(4-Methylphenyl)[1-(pentafluorophenyl)-5-(trifluoromethyl)-1*H*-1,2,3-triazol-4-yl]methanone: A mixture of the corresponding 4,4,4-trifluoro-1-(*p*-tolyl)butane-1,3-dione 230 mg (1.00 mmol), 1-azido-2,3,4,5,6-pentafluorobenzene 209 mg (1.00 mmol), and triethylamine (0.43 ml, 3.00 mmol) was heated at 343–353 K for 3 h. Volatiles were evaporated *in vacuo* and the residue was purified by column chromatography on silica gel using dichloromethane as an eluent. Colourless crystals were grown by slow evaporation of a dichloromethane solution, yield 21%; m.p. 391–394 K; ^{1}H NMR (500 MHz, DMSO-d_6) δ 8.02 (*d*, *J* = 7.9 Hz, 2H, H^{Ar}-2,6), 7.44 (*d*, *J* = 7.8 Hz, 2H, H^{Ar}-3,5), 2.43 (*s*, 3H); ^{13}C NMR (126 MHz, DMSO-d_6) δ 183.74 (CO), 145.73 (C^{Tol}-4), 145.57 (C^{Triazole}-4), 143.61 (*m*), 141.68 (*m*), 138.84 (*m*), 136.79 (*m*), 132.61 (C^{Tol}-1), 130.67 (*q*, *J* = 41.7 Hz, C^{Triazole}-5), 130.63 (2 × C^{Tol}-2,6), 129.49 (2 × C^{Tol}-3,5), 118.36 (*q*, $^1J_{C-F}$ = 270.9 Hz, CF_3), 109.59 (*m*), 21.37 (CH_3); ^{19}F NMR (376 MHz, DMSO-d_6) δ −58.46 (CF_3), −146.39 (*d*, *J* = 21.5 Hz, 2 × F-2,6), −146.53 (*t*, *J* = 23.4 Hz, F-4), −159.61 (*t*, *J* = 23.3 Hz, 2 × F-3,5); MS, *m*/*z* = 422 (M^+ + 1). Calculated for $C_{17}H_7F_8N_3O$, (%): C, 48.47; H, 1.68; N, 9.98. Found (%): C, 48.55; H, 1.67; N, 9.91.

Table 2
Experimental details.

Crystal data	
Chemical formula	$C_{17}H_7F_8N_3O$
M_r	421.26
Crystal system, space group	Orthorhombic, $P2_12_12_1$
Temperature (K)	150
a, *b*, *c* (Å)	6.7605 (6), 15.065 (1), 16.0849 (9)
V (Å^3)	1638.2 (2)
Z	4
Radiation type	Cu *Kα*
μ (mm^{-1})	1.55
Crystal size (mm)	0.43 × 0.12 × 0.08
Data collection	
Diffractometer	New Gemini, Dual, Cu at home/near, Atlas
Absorption correction	Analytical (*CrysAlis PRO*; Rigaku OD, 2021)
T_{min}, T_{max}	0.320, 0.678
No. of measured, independent and observed [$I > 2\sigma(I)$] reflections	15249, 3187, 2311
R_{int}	0.088
(sin $\theta/\lambda)_{max}$ (Å^{-1})	0.618
Refinement	
$R[F^2 > 2\sigma(F^2)]$, $wR(F^2)$, *S*	0.047, 0.109, 1.03
No. of reflections	3187
No. of parameters	264
H-atom treatment	H-atom parameters constrained
$\Delta\rho_{max}$, $\Delta\rho_{min}$ (e Å^{-3})	0.18, −0.18
Absolute structure	Refined as an inversion twin.
Absolute structure parameter	0.2 (3)

Computer programs: *CrysAlis PRO* (Rigaku OD, 2021), *SHELXT* (Sheldrick, 2015*a*), *SHELXL2018/3* (Sheldrick, 2015*b*) and *OLEX2* (Dolomanov *et al.*, 2009).

7. Refinement

Crystal data, data collection and structure refinement details are summarized in Table 2. All H atoms were positioned geometrically with C—H = 0.95–0.98 Å and refined as riding atoms. The constraint U_{iso}(H) = 1.2U_{eq}(carrier) or 1.5U_{eq}(C-methyl carrier) was applied in all cases.

Funding information

This work was supported by the Ministry of Education and Science of Ukraine (grant 'Donor-substituted derivatives of 1,2,3-triazole as materials for organic light emitting diodes').

References

Abdel-Wahab, B. F., Mohamed, H. A., Ng, S. W. & Tiekink, E. R. T. (2013). *Acta Cryst.* E**69**, o638.
Berry, M. T., Castrejon, D. & Hein, J. E. (2014). *Org. Lett.* **16**, 3676–3679.
Birkenfelder, I., Gurke, J., Grubert, L., Hecht, S. & Schmidt, B. M. (2017). *Chem. Asian J.* **12**, 3156–3161.
Blastik, Z. E., Klepetářová, B. & Beier, P. (2018). *ChemistrySelect*, **3**, 7045–7048.
Bunev, A. S., Troshina, M. A., Ostapenko, G. I., Pavlova, A. P. & Khrustalev, V. N. (2014). *Acta Cryst.* E**70**, o818.
Danence, L. J. T., Gao, Y., Li, M., Huang, Y. & Wang, J. (2011). *Chem. Eur. J.* **17**, 3584–3587.

Danyliv, I., Danyliv, Y., Lytvyn, R., Bezvikonnyi, O., Volyniuk, D., Simokaitiene, J., Ivaniuk, K., Tsiko, U., Tomkeviciene, A., Dabulienė, A., Skuodis, E., Stakhira, P. & Grazulevicius, J. V. (2021). *Dyes Pigments*, **193**, 109493.

Dolomanov, O. V., Bourhis, L. J., Gildea, R. J., Howard, J. A. K. & Puschmann, H. (2009). *J. Appl. Cryst.* **42**, 339–341.

El-Hiti, G. A., Abdel-Wahab, B. F., Alotaibi, M. H., Hegazy, A. S. & Kariuki, B. M. (2017). *IUCrData*, **2**, x171782.

El-Hiti, G. A., Abdel-Wahab, B. F., Alotaibi, M. H., Hegazy, A. S. & Kariuki, B. M. (2018). *IUCrData*, **3**, x171841.

Feng, Z., Chong, Y., Tang, S., Ruan, H., Fang, Y., Zhao, Y., Jiang, J. & Wang, X. (2021). *Chin. J. Chem.* **39**, 1297–1302.

Fernández-Hernández, J. M., Beltrán, J. I., Lemaur, V., Gálvez-López, M. D., Chien, C. H., Polo, F., Orselli, E., Fröhlich, R., Cornil, J. & De Cola, L. (2013). *Inorg. Chem.* **52**, 1812–1824.

Funabiki, K., Yamada, K., Matsueda, H., Arisawa, Y., Agou, T., Kubota, Y., Inuzuka, T. & Wasada, H. (2021). *Eur. J. Org. Chem.* pp. 1344–1350.

Gavlik, K. D., Sukhorukova, E. S., Shafran, Y. M., Slepukhin, P. A., Benassi, E. & Belskaya, N. P. (2017). *Dyes Pigments*, **136**, 229–242.

Groom, C. R., Bruno, I. J., Lightfoot, M. P. & Ward, S. C. (2016). *Acta Cryst.* B**72**, 171–179.

He, X., Borau-Garcia, J., Woo, A. Y., Trudel, S. & Baumgartner, T. (2013). *J. Am. Chem. Soc.* **135**, 1137–1147.

He, X., Zhang, P., Lin, J. B., Huynh, H. V., Navarro Muñoz, S. E., Ling, C. C. & Baumgartner, T. (2013). *Org. Lett.* **15**, 5322–5325.

Hladka, I., Volyniuk, D., Bezvikonnyi, O., Kinzhybalo, V., Bednarchuk, T. J., Danyliv, Y., Lytvyn, R., Lazauskas, A. & Grazulevicius, J. V. (2018). *J. Mater. Chem. C.* **6**, 13179–13189.

Ichikawa, M., Mochizuki, S., Jeon, H. G., Hayashi, S., Yokoyama, N. & Taniguchi, Y. (2011). *J. Mater. Chem.* **21**, 11791–11799.

Kandhadi, J., Yan, W. C., Cheng, F., Wang, H. & Liu, H. Y. (2018). *New J. Chem.* **42**, 9987–9999.

Kloss, F., Köhn, U., Jahn, B. O., Hager, M. D., Görls, H. & Schubert, U. S. (2011). *Chem. Asian J.* **6**, 2816–2824.

Krivopalov, V. P. & Shkurko, O. P. (2005). *Russ. Chem. Rev.* **74**, 339–379.

Lavoie, K. D., Frauhiger, B. E., White, P. S. & Templeton, J. L. (2017). *J. Mol. Catal. A Chem.* **426**, 474–489.

Li, W., Du, Z., Huang, J., Jia, Q., Zhang, K. & Wang, J. (2014). *Green Chem.* **16**, 3003–3006.

Liu, S., Müller, P., Takase, M. K. & Swager, T. M. (2011). *Inorg. Chem.* **50**, 7598–7609.

Lu, B. Y., Li, Z. M., Zhu, Y. Y., Zhao, X. & Li, Z. T. (2012). *Tetrahedron*, **68**, 8857–8862.

Lukeš, V., Michalík, M., Poliak, P., Cagardová, D., Végh, D., Bortňák, D., Fronc, M. & Kožíšek, J. (2016). *Synth. Met.* **219**, 83–92.

Matsui, M., Suzuki, M., Nunome, I., Kubota, Y., Funabiki, K., Shiro, M., Matsumoto, S. & Shiozaki, H. (2008). *Tetrahedron*, **64**, 8830–8836.

Maugeri, L., Asencio-Hernández, J., Lébl, T., Cordes, D. B., Slawin, A. M., Delsuc, M. A. & Philp, D. (2016). *Chem. Sci.* **7**, 6422–6428.

Maugeri, L., Lébl, T., Cordes, D. B., Slawin, A. M. & Philp, D. (2017). *J. Org. Chem.* **82**, 1986–1995.

Milo, A., Neel, A. J., Toste, F. D. & Sigman, M. S. (2015). *Science*, **347**, 737–743.

Mohamed, H. A., Alotaibi, H. A., Kariuki, B. M. & El-Hiti, G. A. (2021). CSD Communication (CCDC 1861196). CCDC, Cambridge, England. https://doi.org/10.5517/ccdc.csd.cc20gqlt.

Moseev, T. D., Varaksin, M. V., Gorlov, D. A., Nikiforov, E. A., Kopchuk, D. S., Starnovskaya, E. S., Khasanov, A. F., Zyryanov, G. V., Charushin, V. N. & Chupakhin, O. N. (2019). *J. Fluor. Chem.* **224**, 89–99.

Pokhodylo, N. T. & Obushak, M. D. (2019). *Russ. J. Org. Chem.* **55**, 1241–1243.

Pokhodylo, N. T. & Shyyka, O. Y. (2017). *Synth. Commun.* **47**, 1096–1101.

Pokhodylo, N. T., Shyyka, O. Y., Goreshnik, E. A. & Obushak, M. D. (2020). *ChemistrySelect*, **5**, 260–264.

Pokhodylo, N. T., Shyyka, O. Y., Matiychuk, V. S., Obushak, M. D. & Pavlyuk, V. V. (2017). *ChemistrySelect*, **2**, 5871–5876.

Pokhodylo, N. T., Shyyka, O. Y. & Obushak, M. D. (2014). *Synth. Commun.* **44**, 1002–1006.

Pokhodylo, N. T., Shyyka, O. Y. & Obushak, M. D. (2018). *Chem. Heterocycl. Compd*, **54**, 773–779.

Ramachary, D. B., Ramakumar, K. & Narayana, V. V. (2008). *Chem. Eur. J.* **14**, 9143–9147.

Rigaku OD (2021). *CrysAlis PRO*. Rigaku Oxford Diffraction, Tokyo, Japan.

Rillahan, C. D., Schwartz, E., McBride, R., Fokin, V. V. & Paulson, J. C. (2012). *Angew. Chem. Int. Ed.* **51**, 11014–11018.

Rozin, Y. A., Leban, J., Dehaen, W., Nenajdenko, V. G., Muzalevskiy, V. M., Eltsov, O. S. & Bakulev, V. A. (2012). *Tetrahedron*, **68**, 614–618.

Shafran, Y. M., Beryozkina, T. V., Efimov, I. V. & Bakulev, V. A. (2019). *Chem. Heterocycl. Compd*, **55**, 704–715.

Sheldrick, G. M. (2015*a*). *Acta Cryst.* A**71**, 3–8.

Sheldrick, G. M. (2015*b*). *Acta Cryst.* C**71**, 3–8.

Singh, S., El-Sakkary, N., Skinner, D. E., Sharma, P. P., Ottilie, S., Antonova-Koch, Y., Kumar, P., Winzeler, E., Caffrey, C. R. & Rathi, B. (2020). *Pharmaceuticals*, **13**, 25. https://doi.org/10.3390/ph13020025.

Spackman, M. A. & Jayatilaka, D. (2009). *CrystEngComm*, **11**, 19–32.

Tomkute-Luksiene, D., Keruckas, J., Malinauskas, T., Simokaitiene, J., Getautis, V., Grazulevicius, J. V., Volyniuk, D., Cherpak, V., Stakhira, P., Yashchuk, V., Kosach, V., Luka, G. & Sidaravicius, J. (2013). *Dyes Pigments*, **96**, 278–286.

Turner, M. J., Mckinnon, J. J., Wolff, S. K., Grimwood, D. J., Spackman, P. R., Jayatilaka, D. & Spackman, M. A. (2017). *CrystalExplorer17*. The University of Western Australia. http://hirshfeldsurface.net

Vinutha, N., Madan Kumar, S., Nithinchandra, Balakrishna, K., Lokanath, N. K. & Revannasiddaiah, D. (2013). *Acta Cryst.* E**69**, o1724.

Wang, C., Li, G. & Zhang, Q. (2013). *Tetrahedron Lett.* **54**, 2633–2636.

Xie, S., Lopez, S. A., Ramström, O., Yan, M. & Houk, K. N. (2015). *J. Am. Chem. Soc.* **137**, 2958–2966.

Zeghada, S., Bentabed-Ababsa, G., Derdour, A., Abdelmounim, S., Domingo, L. R., Sáez, J. A., Roisnel, T., Nassar, E. & Mongin, F. (2011). *Org. Biomol. Chem.* **9**, 4295–4305.

Zukerman-Schpector, J., Dias, C. da S., Schwab, R. S., Jotani, M. M. & Tiekink, E. R. T. (2018). *Acta Cryst.* E**74**, 1195–1200.

supporting information

Acta Cryst. (2021). E**77**, 1067-1071 [https://doi.org/10.1107/S2056989021010070]

Synthesis, crystal structure and Hirshfeld surface analysis of (4-methylphenyl)[1-(pentafluorophenyl)-5-(trifluoromethyl)-1*H*-1,2,3-triazol-4-yl]methanone

Nazariy T. Pokhodylo, Yurii Slyvka, Evgeny Goreshnik and Roman Lytvyn

Computing details

Data collection: *CrysAlis PRO* (Rigaku OD, 2021); cell refinement: *CrysAlis PRO* (Rigaku OD, 2021); data reduction: *CrysAlis PRO* (Rigaku OD, 2021); program(s) used to solve structure: SHELXT (Sheldrick, 2015a); program(s) used to refine structure: *SHELXL2018/3* (Sheldrick, 2015b); molecular graphics: *OLEX2* (Dolomanov *et al.*, 2009); software used to prepare material for publication: *OLEX2* (Dolomanov *et al.*, 2009).

(4-Methylphenyl)[1-(pentafluorophenyl)-5-(trifluoromethyl)-1*H*-1,2,3-triazol-4-yl]methanone

Crystal data

$C_{17}H_7F_8N_3O$
$M_r = 421.26$
Orthorhombic, $P2_12_12_1$
$a = 6.7605$ (6) Å
$b = 15.065$ (1) Å
$c = 16.0849$ (9) Å
$V = 1638.2$ (2) Å^3
$Z = 4$
$F(000) = 840$
$D_x = 1.708$ Mg m^{-3}
Cu $K\alpha$ radiation, $\lambda = 1.54184$ Å
Cell parameters from 2646 reflections
$\theta = 4.0$–$72.2°$
$\mu = 1.55$ mm^{-1}
$T = 150$ K
Irregular, colourless
0.43 × 0.12 × 0.08 mm

Data collection

New Gemini, Dual, Cu at home/near, Atlas diffractometer
Detector resolution: 10.6426 pixels mm^{-1}
ω scans
Absorption correction: analytical (CrysalisPro; Rigaku OD, 2021)
$T_{min} = 0.320$, $T_{max} = 0.678$
15249 measured reflections
3187 independent reflections
2311 reflections with $I > 2\sigma(I)$
$R_{int} = 0.088$
$\theta_{max} = 72.3°$, $\theta_{min} = 4.0°$
$h = -7\rightarrow8$
$k = -18\rightarrow18$
$l = -19\rightarrow19$

Refinement

Refinement on F^2
Least-squares matrix: full
$R[F^2 > 2\sigma(F^2)] = 0.047$
$wR(F^2) = 0.109$
$S = 1.03$
3187 reflections
264 parameters
0 restraints
Hydrogen site location: inferred from neighbouring sites
H-atom parameters constrained
$w = 1/[\sigma^2(F_o^2) + (0.031P)^2 + 0.1487P]$ where $P = (F_o^2 + 2F_c^2)/3$
$(\Delta/\sigma)_{max} < 0.001$
$\Delta\rho_{max} = 0.18$ e Å^{-3}
$\Delta\rho_{min} = -0.18$ e Å^{-3}
Absolute structure: Refined as an inversion twin.
Absolute structure parameter: 0.2 (3)

Special details

Geometry. All esds (except the esd in the dihedral angle between two l.s. planes) are estimated using the full covariance matrix. The cell esds are taken into account individually in the estimation of esds in distances, angles and torsion angles; correlations between esds in cell parameters are only used when they are defined by crystal symmetry. An approximate (isotropic) treatment of cell esds is used for estimating esds involving l.s. planes.

Refinement. Refined as a 2-component inversion twin.

Fractional atomic coordinates and isotropic or equivalent isotropic displacement parameters (Å²)

	x	*y*	*z*	U_{iso}*/U_{eq}
F1	0.0932 (5)	0.4231 (2)	0.51007 (19)	0.0563 (9)
F2	0.2755 (6)	0.52826 (18)	0.4634 (2)	0.0575 (10)
F3	0.1757 (5)	0.42585 (19)	0.38129 (17)	0.0456 (8)
F4	0.5987 (6)	0.50612 (18)	0.33789 (17)	0.0565 (9)
F5	0.6160 (6)	0.5157 (2)	0.16979 (18)	0.0609 (10)
F6	0.5614 (6)	0.3674 (3)	0.07762 (16)	0.0612 (10)
F7	0.4985 (6)	0.2089 (2)	0.15264 (18)	0.0566 (9)
F8	0.4847 (5)	0.19857 (17)	0.32018 (16)	0.0456 (8)
O1	0.3633 (7)	0.4664 (2)	0.6435 (2)	0.0496 (10)
N1	0.5368 (7)	0.3474 (2)	0.4207 (2)	0.0351 (10)
N2	0.6809 (7)	0.2985 (3)	0.4582 (2)	0.0418 (11)
N3	0.6565 (8)	0.3072 (3)	0.5387 (2)	0.0410 (10)
C1	0.5367 (8)	0.3525 (3)	0.3316 (3)	0.0339 (11)
C2	0.5726 (8)	0.4330 (3)	0.2930 (3)	0.0396 (12)
C3	0.5793 (9)	0.4382 (4)	0.2066 (3)	0.0451 (13)
C4	0.5531 (9)	0.3623 (4)	0.1611 (3)	0.0430 (13)
C5	0.5215 (9)	0.2822 (3)	0.1983 (3)	0.0405 (12)
C6	0.5130 (8)	0.2771 (3)	0.2847 (3)	0.0357 (11)
C7	0.4210 (8)	0.3878 (3)	0.4781 (3)	0.0319 (11)
C8	0.4981 (8)	0.3615 (3)	0.5531 (3)	0.0337 (11)
C9	0.4375 (9)	0.3934 (3)	0.6379 (3)	0.0385 (13)
C10	0.4732 (8)	0.3363 (3)	0.7117 (3)	0.0345 (11)
C11	0.5049 (8)	0.2451 (3)	0.7063 (3)	0.0340 (10)
H11	0.509418	0.217046	0.653465	0.041*
C12	0.5297 (8)	0.1955 (3)	0.7776 (3)	0.0360 (11)
H12	0.549256	0.133197	0.773331	0.043*
C13	0.5267 (8)	0.2352 (3)	0.8560 (3)	0.0374 (12)
C14	0.4964 (10)	0.3264 (3)	0.8609 (3)	0.0454 (14)
H14	0.494442	0.354584	0.913774	0.054*
C15	0.4693 (9)	0.3765 (3)	0.7897 (3)	0.0438 (14)
H15	0.447771	0.438645	0.794080	0.053*
C16	0.5547 (10)	0.1808 (3)	0.9339 (3)	0.0493 (16)
H16A	0.562191	0.117776	0.919256	0.074*
H16B	0.442677	0.190607	0.971434	0.074*
H16C	0.677506	0.198827	0.961531	0.074*
C17	0.2417 (9)	0.4415 (3)	0.4588 (3)	0.0405 (12)

Atomic displacement parameters (Å²)

	U^{11}	U^{22}	U^{33}	U^{12}	U^{13}	U^{23}
F1	0.045 (2)	0.0728 (19)	0.0511 (16)	0.0166 (18)	0.0065 (16)	0.0039 (15)
F2	0.077 (3)	0.0330 (13)	0.0620 (18)	0.0102 (16)	−0.0228 (18)	−0.0058 (14)
F3	0.049 (2)	0.0459 (15)	0.0416 (14)	0.0086 (15)	−0.0134 (14)	−0.0077 (12)
F4	0.084 (3)	0.0395 (15)	0.0464 (15)	−0.0048 (17)	0.0019 (16)	0.0027 (13)
F5	0.073 (3)	0.0606 (18)	0.0492 (16)	−0.001 (2)	0.0050 (17)	0.0228 (15)
F6	0.061 (3)	0.094 (2)	0.0285 (13)	0.005 (2)	−0.0016 (15)	0.0040 (14)
F7	0.058 (2)	0.0650 (18)	0.0470 (15)	−0.001 (2)	−0.0009 (17)	−0.0199 (14)
F8	0.050 (2)	0.0372 (13)	0.0497 (15)	−0.0019 (16)	0.0064 (15)	−0.0027 (11)
O1	0.072 (3)	0.0354 (17)	0.0412 (18)	0.0107 (19)	0.0010 (19)	0.0006 (14)
N1	0.040 (3)	0.0344 (18)	0.0312 (17)	0.005 (2)	−0.0025 (19)	0.0008 (15)
N2	0.042 (3)	0.049 (2)	0.0345 (19)	0.008 (2)	0.0005 (19)	0.0094 (19)
N3	0.042 (3)	0.050 (2)	0.0316 (19)	0.004 (2)	0.0010 (19)	0.0040 (17)
C1	0.031 (3)	0.041 (2)	0.030 (2)	0.004 (2)	−0.002 (2)	0.0003 (18)
C2	0.042 (3)	0.038 (2)	0.039 (2)	0.004 (3)	−0.001 (2)	0.000 (2)
C3	0.046 (3)	0.053 (3)	0.037 (2)	0.001 (3)	0.003 (2)	0.016 (2)
C4	0.037 (4)	0.067 (3)	0.026 (2)	0.008 (3)	0.002 (2)	0.002 (2)
C5	0.030 (3)	0.053 (3)	0.038 (2)	0.002 (3)	−0.003 (2)	−0.008 (2)
C6	0.026 (3)	0.039 (2)	0.041 (2)	0.002 (2)	0.002 (2)	0.0021 (19)
C7	0.037 (3)	0.0276 (19)	0.031 (2)	−0.002 (2)	0.000 (2)	0.0012 (17)
C8	0.032 (3)	0.034 (2)	0.035 (2)	−0.002 (2)	0.000 (2)	0.0018 (17)
C9	0.046 (4)	0.037 (2)	0.032 (2)	0.002 (2)	−0.003 (2)	0.0021 (19)
C10	0.036 (3)	0.039 (2)	0.0285 (19)	0.001 (2)	0.000 (2)	0.0009 (17)
C11	0.030 (3)	0.039 (2)	0.033 (2)	0.002 (2)	0.000 (2)	−0.0025 (17)
C12	0.034 (3)	0.038 (2)	0.036 (2)	0.003 (2)	0.001 (2)	0.0006 (18)
C13	0.035 (3)	0.045 (2)	0.032 (2)	0.009 (2)	−0.004 (2)	0.0030 (18)
C14	0.058 (4)	0.047 (3)	0.031 (2)	0.011 (3)	−0.001 (3)	−0.0058 (19)
C15	0.049 (4)	0.045 (3)	0.037 (2)	0.012 (3)	−0.007 (3)	−0.005 (2)
C16	0.061 (5)	0.052 (3)	0.036 (2)	0.014 (3)	−0.001 (3)	0.005 (2)
C17	0.050 (4)	0.038 (2)	0.034 (2)	0.007 (3)	−0.006 (2)	−0.004 (2)

Geometric parameters (Å, º)

F1—C17	1.328 (7)	C5—C6	1.393 (6)
F2—C17	1.329 (6)	C7—C8	1.373 (6)
F3—C17	1.345 (6)	C7—C17	1.490 (8)
F4—C2	1.328 (6)	C8—C9	1.502 (6)
F5—C3	1.332 (6)	C9—C10	1.485 (6)
F6—C4	1.346 (5)	C10—C11	1.393 (6)
F7—C5	1.336 (6)	C10—C15	1.394 (6)
F8—C6	1.328 (5)	C11—H11	0.9500
O1—C9	1.213 (6)	C11—C12	1.380 (6)
N1—N2	1.362 (6)	C12—H12	0.9500
N1—C1	1.435 (5)	C12—C13	1.395 (6)
N1—C7	1.355 (6)	C13—C14	1.392 (7)
N2—N3	1.313 (6)	C13—C16	1.508 (6)

N3—C8	1.368 (7)	C14—H14	0.9500
C1—C2	1.384 (7)	C14—C15	1.384 (7)
C1—C6	1.373 (7)	C15—H15	0.9500
C2—C3	1.393 (7)	C16—H16A	0.9800
C3—C4	1.369 (8)	C16—H16B	0.9800
C4—C5	1.363 (8)	C16—H16C	0.9800

N2—N1—C1	118.1 (4)	C10—C9—C8	119.7 (4)
C7—N1—N2	110.8 (4)	C11—C10—C9	123.1 (4)
C7—N1—C1	131.0 (4)	C11—C10—C15	119.1 (4)
N3—N2—N1	107.1 (4)	C15—C10—C9	117.7 (4)
N2—N3—C8	109.0 (4)	C10—C11—H11	119.9
C2—C1—N1	119.6 (4)	C12—C11—C10	120.1 (4)
C6—C1—N1	120.4 (4)	C12—C11—H11	119.9
C6—C1—C2	119.9 (4)	C11—C12—H12	119.4
F4—C2—C1	120.4 (4)	C11—C12—C13	121.1 (4)
F4—C2—C3	119.4 (5)	C13—C12—H12	119.4
C1—C2—C3	120.1 (5)	C12—C13—C16	121.0 (4)
F5—C3—C2	119.9 (5)	C14—C13—C12	118.5 (4)
F5—C3—C4	121.2 (4)	C14—C13—C16	120.5 (4)
C4—C3—C2	118.9 (5)	C13—C14—H14	119.6
F6—C4—C3	118.7 (5)	C15—C14—C13	120.7 (4)
F6—C4—C5	119.7 (5)	C15—C14—H14	119.6
C5—C4—C3	121.6 (4)	C10—C15—H15	119.8
F7—C5—C4	120.6 (4)	C14—C15—C10	120.4 (4)
F7—C5—C6	119.8 (5)	C14—C15—H15	119.8
C4—C5—C6	119.6 (5)	C13—C16—H16A	109.5
F8—C6—C1	121.1 (4)	C13—C16—H16B	109.5
F8—C6—C5	119.0 (4)	C13—C16—H16C	109.5
C1—C6—C5	119.9 (4)	H16A—C16—H16B	109.5
N1—C7—C8	104.5 (4)	H16A—C16—H16C	109.5
N1—C7—C17	124.9 (4)	H16B—C16—H16C	109.5
C8—C7—C17	130.4 (4)	F1—C17—F2	107.5 (4)
N3—C8—C7	108.7 (4)	F1—C17—F3	106.8 (5)
N3—C8—C9	123.9 (4)	F1—C17—C7	111.9 (4)
C7—C8—C9	127.0 (5)	F2—C17—F3	106.3 (4)
O1—C9—C8	118.0 (4)	F2—C17—C7	112.5 (5)
O1—C9—C10	122.2 (4)	F3—C17—C7	111.6 (4)

F4—C2—C3—F5	1.5 (9)	C2—C1—C6—F8	177.8 (5)
F4—C2—C3—C4	179.7 (5)	C2—C1—C6—C5	−1.2 (9)
F5—C3—C4—F6	−1.2 (9)	C2—C3—C4—F6	−179.4 (5)
F5—C3—C4—C5	178.0 (6)	C2—C3—C4—C5	−0.3 (10)
F6—C4—C5—F7	−0.1 (9)	C3—C4—C5—F7	−179.3 (6)
F6—C4—C5—C6	180.0 (5)	C3—C4—C5—C6	0.9 (10)
F7—C5—C6—F8	0.9 (9)	C4—C5—C6—F8	−179.2 (5)
F7—C5—C6—C1	−180.0 (5)	C4—C5—C6—C1	−0.1 (9)
O1—C9—C10—C11	161.5 (6)	C6—C1—C2—F4	−179.0 (5)

O1—C9—C10—C15	−16.8 (9)	C6—C1—C2—C3	1.8 (9)
N1—N2—N3—C8	−0.2 (6)	C7—N1—N2—N3	0.4 (6)
N1—C1—C2—F4	−2.9 (9)	C7—N1—C1—C2	61.7 (8)
N1—C1—C2—C3	177.9 (5)	C7—N1—C1—C6	−122.2 (6)
N1—C1—C6—F8	1.8 (9)	C7—C8—C9—O1	−25.4 (9)
N1—C1—C6—C5	−177.3 (5)	C7—C8—C9—C10	155.8 (5)
N1—C7—C8—N3	0.3 (5)	C8—C7—C17—F1	−37.5 (7)
N1—C7—C8—C9	174.0 (5)	C8—C7—C17—F2	83.6 (7)
N1—C7—C17—F1	136.6 (5)	C8—C7—C17—F3	−157.0 (5)
N1—C7—C17—F2	−102.3 (5)	C8—C9—C10—C11	−19.9 (9)
N1—C7—C17—F3	17.1 (7)	C8—C9—C10—C15	161.9 (5)
N2—N1—C1—C2	−114.2 (6)	C9—C10—C11—C12	−177.5 (5)
N2—N1—C1—C6	61.9 (7)	C9—C10—C15—C14	178.3 (6)
N2—N1—C7—C8	−0.4 (5)	C10—C11—C12—C13	−0.9 (9)
N2—N1—C7—C17	−175.8 (4)	C11—C10—C15—C14	0.0 (9)
N2—N3—C8—C7	−0.1 (6)	C11—C12—C13—C14	0.5 (9)
N2—N3—C8—C9	−174.1 (5)	C11—C12—C13—C16	−179.7 (6)
N3—C8—C9—O1	147.4 (5)	C12—C13—C14—C15	0.2 (10)
N3—C8—C9—C10	−31.3 (8)	C13—C14—C15—C10	−0.5 (10)
C1—N1—N2—N3	177.1 (4)	C15—C10—C11—C12	0.7 (9)
C1—N1—C7—C8	−176.5 (5)	C16—C13—C14—C15	−179.5 (6)
C1—N1—C7—C17	8.1 (8)	C17—C7—C8—N3	175.3 (5)
C1—C2—C3—F5	−179.3 (5)	C17—C7—C8—C9	−11.0 (9)
C1—C2—C3—C4	−1.1 (10)		

Hydrogen-bond geometry (Å, º)

D—H···*A*	*D*—H	H···*A*	*D*···*A*	*D*—H···*A*
C11—H11···F3^{i}	0.95	2.49	3.155 (5)	127
C15—H15···F3^{ii}	0.95	2.61	3.463 (6)	149
C16—H16*A*···F2^{iii}	0.98	2.57	3.054 (6)	111
C16—H16*A*···O1^{iii}	0.98	2.54	3.505 (6)	167

Symmetry codes: (i) *x*+1/2, −*y*+1/2, −*z*+1; (ii) −*x*+1/2, −*y*+1, *z*+1/2; (iii) −*x*+1, *y*−1/2, −*z*+3/2.